Mapping of Kinematic and Dynamic Parameters for Coupled Manipulators

Zhiming Ji

Ming C. Leu

Department of Mechanical and Industrial Engineering, New Jersey Institute of Technology, Newark, NJ 07102

Industrial manipulators use various types of transmissions, such as gears, belts, chains, and parallel mechanisms, to transmit driving power to the links. By arrangement many such transmissions cause coupled joint motions. Manipulators having coupled joint motions are referred to as coupled manipulators. Conventional methods for constructing Jacobian matrix and compliance matrix are not directly applicable to coupled manipulators. The concept of the mapping matrix is used in this paper for establishing relationships of torque, speed, Jacobian and compliance of these manipulators with those obtained with conventional methods. A method of constructing the mapping matrix systematically is discussed. Two examples show that the proposed method is easy to implement.

1 Introduction

As the demand on more accurate robots increases, study of robot compliance and its effect on robot positioning accuracy has become of greater interest. Experimental evidence [1] indicates that for most existing manipulators, the compliance of the manipulator is primarily a result of compliant joints. The major source of the joint compliance occurs in transmissions, reducers, and servo drive systems [2]. Compliance matrix [3] has been used to describe the relation between an applied load and the deflection of the end-effector due to joint compliance. If joint i has a stiffness as k_i ($i = 1, \ldots, n$), then we can construct a diagonal stiffness matrix

$$K = diag[k_1, k_2, \cdots, k_n] \tag{1}$$

and the effective end-effector compliance matrix

$$C_e = JK^{-1}J^T \tag{2}$$

where J is the conventional Jacobian matrix of a manipulator. By conventional, we mean that the *relative* joint displacements have been chosen to be the set of generalized coordinates and that the Jacobian is calculated with respect to this set of generalized coordinates [4–7]. The deflection $\Delta\mathbf{S}$ (a generalized Cartesian displacement vector including both translation and rotation), caused by the joint compliance, of a manipulator end-effector under a load $\mathbf{F}$ (a generalized Cartesian force vector including both force and moment) is simply

$$\Delta\mathbf{S} = C_e\mathbf{F} \tag{3}$$

When a manipulator has a simple actuation structure (that is, it is serial and each of its links is driven by an actuator mounted on the preceding link), the end-effector compliance matrix is easy to find. All we need is to measure the stiffness of each joint and to find the Jacobian matrix. However, finding the joint stiffness matrix corresponding to the conventional Jacobian can become difficult when the actuation structure of a manipulator is not so simple. In many manipulator actuation structures, the motions of some links are coupled and the desired driving torques of the actuators (*i.e.*, torques in actuator space) are not the same as the computed joint torques in joint space. Such manipulators are referred to as *Coupled Manipulators*. Many industrial manipulators, such as IBM 7540/7576 and GE P-50, belong to this category.

Lagrange-Euler and Newton-Euler formulations of robot dynamics, and their variations, have been used to compute joint torque τ with the assumption that the driving actuator of each link is mounted on the immediate preceding link and that those torques are propagated sequentially back along the link chain through interaction [5, 6]. But this is not true for coupled manipulators. The Jacobian and compliance matrices of coupled manipulators also differ from those computed by the conventional methods. Luh and Zheng [9] studied the computation of joint force/torque for industrial robots having closed-chain linkages. Their approach involves cutting open the closed-chain linkage to form tree structured open-chain mechanism and constructing dynamics equations for the virtual open-chain robot with holonomic equality constraints at the cut joint. Such a direct approach for analysis needs to be done on an individual basis. Freudenstein and Yang [10] introduced a systematic method for deriving the displacement equations of gear trains, using the concept of fundamental circuits. Freudenstein et al. [11] extended the analysis to the complex bevel-gear trains. Tsai [12] then showed that the kinematics of a complex bevel-gear train can be studied by applying the matrix transformation to an equivalent open-loop chain. Chang and Tsai [13] introduced the concept of transmission lines and structural matrix for kinematic analysis and synthesis of geared robotic mechanisms. In their study of the design of three jointed two-degree-of-freedom robot fingers, Leaver and McCarthy [14] used coupling matrix for analyzing tendon routing schemes and the driving gear trains. Tsai and Lee [15] studied the kinematic structure of tendon-driven mechanisms using graph

Contributed by the Mechanisms Committee and presented at the Design Technical Conference, Chicago, IL, Sept. 16-19, 1990, of The American Society of Mechanical Engineers. Manuscript received March 1990. Associate Technical Editor: J. M. McCarthy.

theory. They showed that the displacement equations of such mechanisms can be systematically derived from the routing of tendons, using the "structure matrix." The results of the static (kinematic) analysis can be extended for relating torques in joint space to those in actuator space. But there has been no discussion on its usage for mapping other parameters such as Jacobian and compliance matrices.

This paper presents not only a different approach to the previously studied problem, it also addresses computation of Jacobian and compliance matrices for coupled manipulators. We will present a method, derived based on dynamics formulation, for constructing the torque mapping matrix, which is key to all of the relations between speed, Jacobian and compliance in actuator space and the same parameters in joint space. Once this matrix becomes available, torques and Jacobians computed with conventional formulations can be easily transformed into the actual torques and Jacobians of coupled manipulators. The fact that the matrix is derived directly from dynamics formulation ensures its validity for mapping of dynamic parameters. A major feature of this approach is that the mapping matrix can be constructed by inspecting the locations of a manipulator's actuators. This enables the study of the compliance property of a coupled robot without having to disassemble the robot for the information of its kinematic structure. This approach is, however, not applicable to the open-ended tendons where the dimension of the joint space and that of the actuator space are different.

2 Mapping of Parameters between Actuator Space and Joint Space

Let us map τ^*, the torque vector in actuator space, into τ, the torque vector in joint space, with a matrix N

$$\tau = N\tau^* \tag{4}$$

It has been shown [3, 4]

$$\tau = J^T F \tag{5}$$

Let J^* be the Jacobian with respect to the generalized coordinates in actuator space, then it can be shown

$$\tau^* = (J^*)^T F \tag{6}$$

From the above three equations we have

$$J = J^* N^T \tag{7a}$$

$$J^* = JN^{-T} \tag{7b}$$

Let the stiffness of the ith actuator and its transmission in actuator space be k_i^*, then we have another diagonal stiffness matrix $K^* = diag[k_1^*, k_2^*, \cdots, k_n^*]$. The end-effector compliance matrix C_e can be written as

$$C_e = J^* (K^*)^{-1} (J^*)^T \tag{8}$$

Combining Eqs. (2), (7), and (8), we get

$$C_e = JK_{eq}^{-1} J^T \tag{9}$$

where

$$K_{eq} = NK^* N^T \tag{10}$$

is the equivalent stiffness matrix when the conventional Jacobian is used to obtain the end-effector compliance matrix.

Equations (7) and (10) show that the relation between J and J^* and the relation between K_{eq} and K^* both depend on N, the torque mapping matrix from actuator space to joint space. According to the virtual work principle,

$$(\tau^*)^T \dot{\phi} = \tau^T \dot{\theta} \tag{11}$$

where ϕ is the vector of generalized coordinates in actuator space, θ is the vector of generalized coordinates in joint space, and θ and ϕ are their time derivatives. Using Eq. (4), we have

$$\dot{\phi} = N^T \dot{\theta} \tag{12}$$

Equation (12) shows that the torque mapping matrix N is in fact the mapping matrix between joint velocity and actuator velocity. Thus, matrix N plays an important role in mapping between variables represented in the two different sets of generalized coordinates. For a simple manipulator, the joint torques are the same as the actuator torques: In this case, N is an identity matrix and $K_{eq} = K^*$. This is not the case in coupled manipulators, however. For example, in many manipulator designs some actuators are installed at or near the base of a manipulator so that one actuator does not act as load to other actuators. (There are other reasons, of course, for doing this.) That means not all the joint torques are propagated sequentially back along the link chain. Converting joint torques to actuator torques becomes a coupled mapping. To gain an insight on how this mapping can be used for studying the dynamics of a coupled manipulator, a method for constructing this mapping matrix based on dynamics formulation will be given in the next section.

3 Construction of Mapping Matrix, N

We first consider a manipulator with all revolute joints. *If every link of a manipulator is driven by an actuator mounted on its preceding link*, then from the iterative Newton-Euler formulation [5]

$${}^i f_i = {}^i_{i+1}R \, {}^{i+1} f_{i+1} + {}^i F_i \tag{13}$$

$${}^i n_i = {}^i N_i + {}^i_{i+1}R \, {}^{i+1} n_{i+1} + {}^i P_{ci} \times {}^i F_i + {}^i P_{i+1} \times {}^i_{i+1}R \, {}^{i+1} f_{i+1} \tag{14}$$

$$\tau_i = {}^i n_i^T \, {}^i \hat{z}_i \tag{15}$$

where, as shown in Fig. 1,

- ${}^i n_i$ = moment exerted on link i by link $i-1$
- ${}^i f_i$ = force exerted on link i by link $i-1$
- ${}^i N_i$ = inertial moment of link i
- ${}^i F_i$ = inertial force of link i
- ${}^i P_{ci}$ = position vector of the center of mass of link i
- ${}^i P_{i+1}$ = position vector of the origin of frame $\{i+1\}$
- ${}^i_{i+1}R$ = rotation matrix describing frame $\{i+1\}$ relative to frame $\{i\}$
- ${}^i \hat{z}_i$ = axis vector of joint i
- τ_i = computed joint torque for link i

Now suppose link i is actuated by a motor Mi mounted on

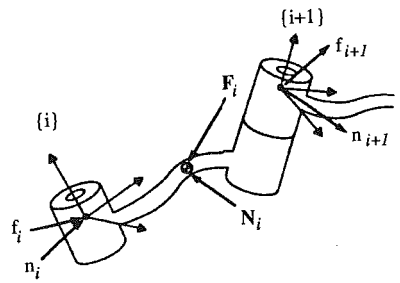

Fig. 1 Forces and moments acting on link i

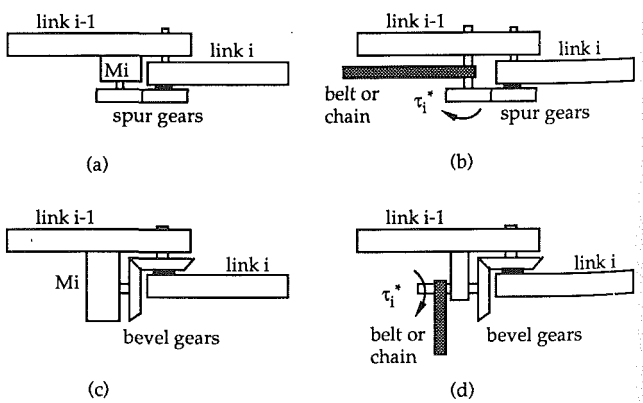

Fig. 2 Effect of replacement of motor *Mi* from link $i-1$ to a link closer to the base

link j ($i-1>j$) and the torque τ_i^* exerted on link i by Mi is transmitted along the link chain to link i. (The transmission ratio is assumed to be one along the path for simplicity.) Such an arrangement changes the actual interaction moments between link i and its adjacent links. The effect of the replacement of motor from link $i-1$ to a link closer to the base is shown in Fig. 2. Figures 2(a) and (c) have motor Mi mounted on link $i-1$. Due to its support of the motor, link $i-1$ receives a reaction torque from the motor. Figures 2(b) and (d) show that the motor has been replaced from link $i-1$. Although link i is still driven by motor Mi, the reaction moment exerted on link $i-1$ by link i has changed. Depending on the type of mechanism used for transmitting torque from motor Mi to link i, the axis of the motor Mi before replacement may or may not be parallel to the joint axis $\hat{z}_i$. If we denote the actual moment exerted on link i by link $i-1$ as ${}^in_i^*$ for the general case, then the moment before the replacement ${}^in_i$ can be related to the moment after the replacement ${}^in_i^*$ as

$$ {}^in_i = {}^in_i^* + \tau_i^* \, {}^i\hat{z}_i^* \tag{16}$$

where ${}^i\hat{z}_i^*$ is the unit vector along the axis of motor Mi before the replacement.

Since reaction moments are propagated backwards, change of motor location from link $i-1$ to link j does not change the torques needed for driving link i and its outer links. Thus

$$ \tau_k^* = \tau_k \quad \text{for } k \geq i \tag{17}$$

With the assumption that motor Mi is mounted on link $i-1$ but the link inertias are calculated based on the actual physical links, the original moment equation for link $i-1$ is

$$ {}^{i-1}n_{i-1} = {}^{i-1}N_{i-1} + {}^{i-1}_iR \, {}^in_i + {}^{i-1}P_{c,i-1} \times {}^{i-1}F_{i-1} + {}^{i-1}P_i \times {}^{i-1}_iR \, {}^if_i \tag{18a}$$

and the actual moment equation (with motor Mi mounted on link j) becomes

$$ {}^{i-1}n_{i-1}^* = {}^{i-1}N_{i-1} + {}^{i-1}_iR \, {}^in_i^* + {}^{i-1}P_{c,i-1} \times {}^{i-1}F_{i-1} + {}^{i-1}P_i \times {}^{i-1}_iR \, {}^if_i \tag{18b}$$

Combining Eqs. (16) and (18), we get

$$ {}^{i-1}n_{i-1} = {}^{i-1}n_{i-1}^* + \tau_i^* \, {}^{i-1}\hat{z}_i^* \tag{19}$$

Multiplying Eq. (19) with ${}^{i-1}\hat{z}_{i-1}$, we obtain

$$ \tau_{i-1} = \tau_{i-1}^* + \tau_i^* ({}^{i-1}\hat{z}_i^*)^T \, {}^{i-1}\hat{z}_{i-1} \tag{20}$$

The same relation holds for all other links between i and j. Therefore, for any link between i and j, we have

$$ \tau_k = \tau_k^* + \tau_i^* ({}^k\hat{z}_i^*)^T \, {}^k\hat{z}_k \quad (j<k<i) \tag{21}$$

But for link j, we have the original moment equation as

$$ {}^jn_j = {}^jN_j + {}^j_{j+1}R \, {}^{j+1}n_{j+1} + {}^jP_{cj} \times {}^jF_j + {}^jP_{j+1} \times {}^j_{j+1}R \, {}^{j+1}f_{j+1} \tag{22a}$$

and its modified form

$$ {}^jn_j^* = {}^jN_j + {}^j_{j+1}R \, {}^{j+1}n_{j+1}^* + {}^jP_{cj} \times {}^jF_j + {}^jP_{j+1} \times {}^j_{j+1}R \, {}^{j+1}f_{j+1} + \tau_i^* \, {}^j\tilde{z}_i \tag{22b}$$

where $\tilde{z}_i$ is the unit vector along the actual axis of motor Mi. Therefore,

$$ \begin{aligned} {}^jn_j &= {}^jn_j^* + {}^j_{j+1}R({}^{j+1}n_{j+1} - {}^{j+1}n_{j+1}^*) - \tau_i^* \, {}^j\tilde{z}_i \\ &\doteq {}^jn_j^* + \tau_i^*({}^j\hat{z}_i^* - {}^j\tilde{z}_i) \end{aligned}$$

Multiplying it with ${}^j\hat{z}_j$, we get

$$ \tau_j = \tau_j^* + \tau_i^*({}^j\hat{z}_i^* - {}^j\tilde{z}_i)^T \, {}^j\hat{z}_j \tag{23}$$

For link $j-1$, we have

$$ {}^{j-1}n_{j-1} = {}^{j-1}n_{j-1}^* + {}^{j-1}_jR({}^jn_j - {}^jn_j^*) = {}^{j-1}n_{j-1}^* + \tau_i^*({}^{j-1}\hat{z}_i^* - {}^{j-1}\tilde{z}_i)$$

Multiplying it with ${}^{j-1}\hat{z}_{j-1}$, we get

$$ \tau_{j-1} = \tau_{j-1}^* + \tau_i^*({}^{j-1}\hat{z}_i^* - {}^{j-1}\tilde{z}_i)^T \, {}^{j-1}\hat{z}_{j-1} \tag{24}$$

The same relation holds for all other links before $j-1$. Therefore, for link j or any link before j,

$$ \tau_k = \tau_k^* + \tau_i^*({}^k\hat{z}_i^* - {}^k\tilde{z}_i)^T \, {}^k\hat{z}_k \quad (k \leq j) \tag{25}$$

Combining Eqs. (17), (21), and (25), we get

$$ \tau_k = \tau_k^* + \tau_i^* b_{ki} \tag{26}$$

with

$$ b_{ki} = \begin{cases} (\hat{z}_i^* - \hat{z}_i)^T \hat{z}_k & k \leq j \\ (\hat{z}_i^*)^T \hat{z}_k & j<k<i \\ 0 & k \geq i \end{cases} \tag{27}$$

The above procedure can be extended to manipulators with m of their links, that is $i = i1, i2, \ldots, im$, having actuators located on links $j1, j2, \ldots, jm$, respectively. The result can be obtained as

$$ \tau_k = \begin{cases} \tau_k^* + \tau_{i1}^* b_{k,i1} + \ldots + \tau_{im}^* b_{k,im} & k<i1 \\ \tau_k^* + \tau_{i2}^* b_{k,i2} + \ldots + \tau_{im}^* b_{k,im} & i1 \leq k<i2 \\ \quad\vdots & \quad\vdots \\ \tau_k^* + \tau_{im}^* b_{k,im} & im-1 \leq k<im \\ \tau_k^* & k \geq im \end{cases} \tag{28}$$

where $b_{k,i1}, b_{k,i2}, \ldots, b_{k,im}$ are the same as that defined in Eq. (27), with j replaced by jl and i replaced by il ($1 \leq l \leq m$).

Equation (28) can be used to construct the general torque mapping matrix as:

$$ N = \begin{bmatrix} 1 & b_{1,i1} & b_{1,i2} & b_{1,im} \\ & \ddots & \vdots & \vdots \\ & b_{i1-1,i1} & \vdots & \vdots \\ & 1 & b_{i1,i2} & b_{i1,im} \\ & & \ddots & \vdots \\ & & b_{i2-1,i2} & \vdots \\ & & 1 & b_{i2,im} \\ & & & \ddots \\ & & & b_{im-1,im} \\ & & & 1 \\ & & & & \ddots \\ & & & & & 1 \end{bmatrix} \tag{29}$$

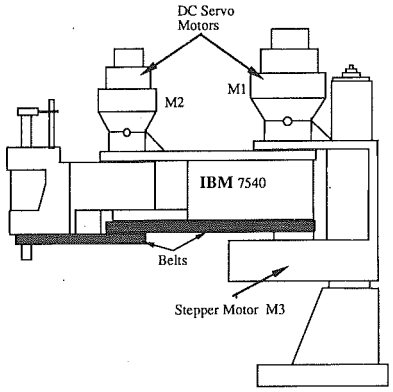

Fig. 3 Drive system of IBM 7540 robot

where all the diagonal elements are 1's and all unmarked elements are 0's if they are not b's. The values of b's could vary according to manipulator configurations. For most industrial manipulators, twist angles are either 0 deg or 90 deg. This property leads to a simpler torque mapping matrix N because the values of b's become constants (either 0 or ± 1).

In the above derivation, we have considered revolute joints. However the formulation can be readily extended to prismatic joints. A prismatic joint should be driven by a rotary actuator with a mechanism, such as a pinion and rack set, to convert rotary motion to linear motion if the joint is to be actuated remotely. If the joint between links $i-1$ and i is prismatic and the joint force is σ_i along the joint axis, then the motor Mi should provide a torque $\tau_i^* = \sigma_i \times r_i$ for driving link i, where r_i is the radius of the pinion used and $\sigma_i = {}^i f_i^{Ti} \hat{z}_i$. After moving motor Mi from link $i-1$ to link j, the force exerted on link i by link $i-1$, ${}^i f_i$, does not change. But the moment exerted on link i by link $i-1$, ${}^i n_i$, changes to ${}^i n_i^*$ as in Eq. (16). Thus, all the above equations still hold.

The mapping matrix N can be determined with Eq. (27) by physically examining the locations of the motors and the directions of the motor axes. Usually, such information is readily available. Once the mapping matrix N is determined, it can be used to transform kinematic and dynamic parameters in conventional formulations to corresponding parameters of coupled manipulators using Eqs. (7), (10), and (12).

The dynamics of a coupled manipulator can be studied as follows. First, the manipulator is treated as a serial manipulator by "disconnecting" all the coupling members (not physically, of course), and a conventional dynamics formulation is applied to this open-chain serial manipulator to obtain joint torques. This technique is similar to that proposed by Luh and Zheng [9]. However, instead of studying the manipulator dynamics by applying a direct formulation to the resultant tree structure, we use mapping to account for the coupling effect. In the case where belts/pulleys or chains/wheels are the coupling members, their masses are still part of the link on which they are mounted. The inertial forces of these elements are calculated based on their motion parameters. Part of the inertial forces is transmitted to the link through bearings and therefore it should be added accordingly to the force and moment equilibrium Eqs. (13) and (14) in the dynamics formulation. The rest of inertial forces of these members (i.e., the part that is not transmitted to links through bearings) becomes additional load to their corresponding motors. If the coupling is caused by closed-chain linkages, the coupling links are not part of the imaginary open-chain serial manipulator, therefore their inertial forces are not considered in this step.

Then the joint torques are mapped into the actuator torques with the mapping matrix N as

$$\tau^* = N^{-1}\tau \tag{30}$$

Finally, additional actuator torques $\Delta\tau^*$ for balancing the remaining inertial forces of the coupling members are computed and added to the total actuator torques. It is straightforward for the case involving belts/pulleys or chains/wheels. For a closed-chain linkage, this can be done by considering its dynamic equilibrium. In this consideration, the links that have been considered in the imaginary open-chain manipulator are treated as massless and the inertial forces of the coupling links are computed based on their known motions and inertial properties. Actuator torques needed for maintaining dynamic equilibrium of the coupling links are then computed and added to the actuator torques obtained in Eq. (30). Two examples are given in the next section illustrating the approach.

4 Examples

As an example, let us look at the drive system of the IBM 7540 robot as shown in Fig. 3. We consider the three revolute joints driven by motors $M1$, $M2$, $M3$. The motor $M3$, which provides the roll motion of the third joint, is located at the base of the robot. Thus, $i = 3$ and $j = 0$. Since the three joints and three motor axes are all parallel, $b_{13} = (\hat{z}_3^*)^T \hat{z}_1 = 1$ and $b_{23} = (\hat{z}_3^*)^T \hat{z}_2 = 1$. The mapping matrix for this case is

$$N = \begin{bmatrix} 1 & 0 & 1 \\ 0 & 1 & 1 \\ 0 & 0 & 1 \end{bmatrix} \tag{31}$$

Substituting Eq. (31) into Eq. (12), we can obtain the following velocity relation:

$$\begin{cases} \dot{\phi}_1 = \dot{\theta}_1 \\ \dot{\phi}_2 = \dot{\theta}_2 \\ \dot{\phi}_3 = \dot{\theta}_1 + \dot{\theta}_2 + \dot{\theta}_3 \end{cases} \tag{32}$$

which has been verified through experimental observations.

The Jacobian matrix corresponding to the position and orientation $[x, y, \phi]$ of the manipulator end-effector on the horizontal plane can be found as

$$J = [J_1 \quad J_2 \quad J_3] = \begin{bmatrix} -(l_1 s_1 + l_2 s_{12}) & -l_2 s_{12} & 0 \\ l_1 c_1 + l_2 c_{12} & l_2 c_{12} & 0 \\ 1 & 1 & 1 \end{bmatrix} \tag{33}$$

and

$$J^* = JN^{-T} = [J_1 - J_3 \quad J_2 - J_3 \quad J_3] = \begin{bmatrix} -(l_1 s_1 + l_2 s_{12}) & -l_2 s_{12} & 0 \\ l_1 c_1 + l_2 c_{12} & l_2 c_{12} & 0 \\ 0 & 0 & 1 \end{bmatrix} \tag{34}$$

where $s_1 \equiv \sin\theta_1$, $c_1 \equiv \cos\theta_1$, $s_{12} \equiv \sin(\theta_1 + \theta_2)$ and $c_{12} \equiv \cos(\theta_1 + \theta_2)$.

With $K^* = \text{diag}[k_1^*, k_2^*, k_3^*]$ and from Eq. (10), we have

$$K_{eq} = \begin{bmatrix} k_1^* + k_3^* & k_3^* & k_3^* \\ k_3^* & k_2^* + k_3^* & k_3^* \\ k_3^* & k_3^* & k_3^* \end{bmatrix} \tag{35}$$

From Eq. (8) or Eq. (9), the elements of the effective end-effector compliance matrix are

$$\begin{aligned} C_{11} &= \frac{(l_1 s_1 + l_2 s_{12})^2}{k_1^*} + \frac{l_2^2 s_{12}^2}{k_2^*} \\ C_{12} = C_{21} &= -\frac{(l_1 s_1 + l_2 s_{12})(l_1 c_1 + l_2 c_{12})}{k_1^*} - \frac{l_2^2 s_{12} c_{12}}{k_2^*} \\ C_{22} &= \frac{(l_1 c_1 + l_2 c_{12})^2}{k_1^*} + \frac{l_2^2 c_{12}^2}{k_2^*} \\ C_{33} &= \frac{1}{k_3^*} \\ C_{13} = C_{31} = C_{23} = C_{32} &= 0 \end{aligned} \tag{36}$$

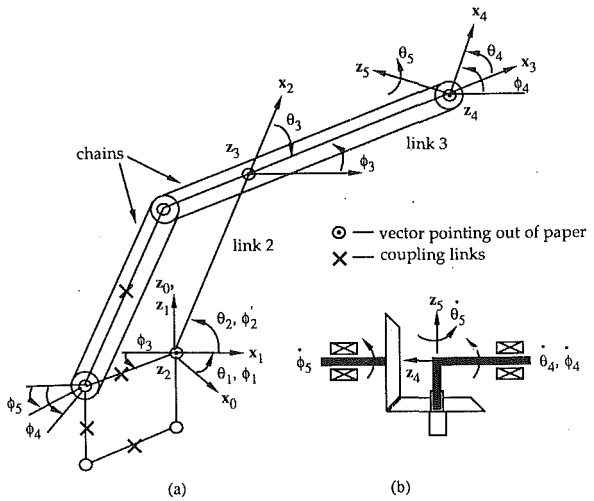

Fig. 4 Drive system of GE P-50 robot

To compute the actuator torques, the belts are "removed." The joint torques τ_1, τ_2, and τ_3 of the resultant "serial robot" are then computed using a conventional dynamics formulation. The inertial forces of the belts and pulleys transmitted to the links through bearings are included in the joint torque computation. Based on the mapping matrix in Eq. (31), the actuator torques are

$$\begin{bmatrix} \tau_1^* \\ \tau_2^* \\ \tau_3^* \end{bmatrix} = N^{-1} \begin{bmatrix} \tau_1 \\ \tau_2 \\ \tau_3 \end{bmatrix} = \begin{bmatrix} \tau_1 - \tau_3 \\ \tau_2 - \tau_3 \\ \tau_3 \end{bmatrix} \tag{37}$$

The rest of inertial forces of the belts and pulleys (i.e., the part that is not transmitted to links through bearings) becomes additional load to motor $M3$, and additional torque $\Delta\tau_3^*$ is then computed for balancing this load.

Another example is the drive system of GE P-50 robot as shown in Fig. 4. One special feature of this type of robot is the parallelogram mechanism, which also exists in the GMF S-series and the ASEA robots.

As we can see from Fig. 4(*a*), link 1 is driven by motor $M1$ mounted on the base, and link 2 is driven by motor $M2$ mounted on link 1. Link 3 is driven by motor $M3$ mounted on link 1 through the parallelogram, therefore the motion of link 3 is coupled to that of link 2. Link 4 and link 5 are driven by motors $M4$ and $M5$, respectively, through transmission chains. Both $M4$ and $M5$ are mounted on a vertical bar in another parallelogram so that their rotations with respect to link 1 are not affected by the rotation of link 3; therefore, they can be treated as mounted on link 1. The motions of links 4 and 5 are shown in Fig. 4(*b*). The i's and j's parameters needed for calculating b's in Eq. (29) are

$$\begin{cases} i1 = 3 \\ j1 = 1 \end{cases} \quad \begin{cases} i2 = 4 \\ j2 = 1 \end{cases} \quad \begin{cases} i3 = 5 \\ j3 = 1 \end{cases}$$

and

$$\hat{z}_2 = \hat{z}_3 = \hat{z}_3^* = \hat{z}_3 = \hat{z}_4 = \hat{z}_4^* = \tilde{z}_4 = \hat{z}_5^* = \tilde{z}_5$$

From Eq. (27), we can obtain

$$b_{13} = b_{14} = b_{15} = 0$$
$$b_{23} = b_{24} = b_{34} = b_{25} = b_{35} = b_{45} = 1$$

Thereore, the mapping matrix for this manipulator is

$$N = \begin{bmatrix} 1 & 0 & 0 & 0 & 0 \\ 0 & 1 & 1 & 1 & 1 \\ 0 & 0 & 1 & 1 & 1 \\ 0 & 0 & 0 & 1 & 1 \\ 0 & 0 & 0 & 0 & 1 \end{bmatrix}. \tag{38}$$

Combining Eq. (38) with Eq. (12), we can work out the following velocity relation:

$$\begin{cases} \dot{\phi}_1 = \dot{\theta}_1 \\ \dot{\phi}_2 = \dot{\theta}_2 \\ \dot{\phi}_3 = \dot{\theta}_3 + \dot{\phi}_2 = \dot{\theta}_3 + \dot{\theta}_2 \\ \dot{\phi}_4 = \dot{\theta}_4 + \dot{\phi}_3 = \dot{\theta}_4 + \dot{\theta}_3 + \dot{\theta}_2 \\ \dot{\phi}_5 = \dot{\theta}_5 + \dot{\phi}_4 = \dot{\theta}_5 + \dot{\theta}_4 + \dot{\theta}_3 + \dot{\theta}_2 \end{cases} \tag{39}$$

which has been experimentally verified to be correct.

The conventional Jacobian for this robot can be found with the vector cross product method [6, 8] as follows:

$${}^0\hat{z}_1 = \begin{bmatrix} 0 \\ 0 \\ 1 \end{bmatrix}, \quad {}^0\hat{z}_2 = {}^0\hat{z}_3 = {}^0\hat{z}_4 = \begin{bmatrix} s_1 \\ -c_1 \\ 0 \end{bmatrix}, \quad {}^0\hat{z}_5 = \begin{bmatrix} -c_1 s_{234} \\ -s_1 s_{234} \\ c_{234} \end{bmatrix},$$

$${}^0P_{1e} = {}^0P_{2e} = \begin{bmatrix} (l_2 c_2 + l_3 c_{23}) c_1 \\ (l_2 c_2 + l_3 c_{23}) s_1 \\ l_2 s_2 + l_3 s_{23} \end{bmatrix},$$

$${}^0P_{3e} = \begin{bmatrix} l_3 c_{23} c_1 \\ l_3 c_{23} s_1 \\ l_3 s_{23} \end{bmatrix}, \quad {}^0P_{4e} = {}^0P_{5e} = \begin{bmatrix} 0 \\ 0 \\ 0 \end{bmatrix}$$

where ${}^0P_{ie}$ is the position of the end-effector from the origin of the ith coordinate frame, expressed in the base coordinate frame.

Thus,

$$J = [J_1 \quad J_2 \quad J_3 \quad J_4 \quad J_5] \tag{40}$$

where

$$J_1 = \begin{bmatrix} {}^0\hat{z}_1 \times {}^0P_{1e} \\ {}^0\hat{z}_1 \end{bmatrix} = \begin{bmatrix} -(l_2 c_2 + l_3 c_{23}) s_1 \\ (l_2 c_2 + l_3 c_{23}) c_1 \\ 0 \\ 0 \\ 0 \\ 1 \end{bmatrix}$$

$$J_2 = \begin{bmatrix} {}^0\hat{z}_2 \times {}^0P_{2e} \\ {}^0\hat{z}_2 \end{bmatrix} = \begin{bmatrix} -(l_2 s_2 + l_3 s_{23}) c_1 \\ (l_2 s_2 + l_3 s_{23}) s_1 \\ l_2 c_2 + l_3 c_{23} \\ s_1 \\ -c_1 \\ 1 \end{bmatrix}$$

$$J_3 = \begin{bmatrix} {}^0\hat{z}_3 \times {}^0P_{3e} \\ {}^0\hat{z}_3 \end{bmatrix} = \begin{bmatrix} -l_3 s_{23} c_1 \\ -l_3 s_{23} s_1 \\ l_3 c_{23} \\ s_1 \\ -c_1 \\ 1 \end{bmatrix}$$

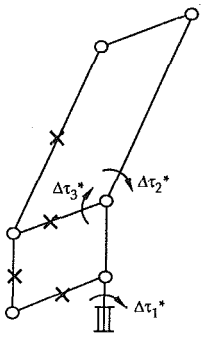

Fig. 5 Dynamics of the coupling parallelgrams

$$J_4 = \begin{bmatrix} {}^0\hat{z}_4 \times {}^0P_{4e} \\ {}^0\hat{z}_4 \end{bmatrix} = \begin{bmatrix} 0 \\ 0 \\ 0 \\ s_1 \\ -c_1 \\ 0 \end{bmatrix}$$

$$J_5 = \begin{bmatrix} {}^0\hat{z}_5 \times {}^0P_{5e} \\ {}^0\hat{z}_5 \end{bmatrix} = \begin{bmatrix} 0 \\ 0 \\ 0 \\ c_1 s_{234} \\ s_1 s_{234} \\ -c_{234} \end{bmatrix}$$

and

$$J^* = JN^{-T} = [J_1 \quad J_2 - J_3 \quad J_3 - J_4 \quad J_4 - J_5 \quad J_5] \qquad (41)$$

Similar to the first example, the transmission chains and the coupling links (marked with × in Fig. 4) are treated as being removed to form an uncoupled serial robot, and its joint torques are computed with a known dynamics formulation. The actuator torques are calculated based on the mapping matrix in Eq. (38) as

$$\begin{bmatrix} \tau_1^* \\ \tau_2^* \\ \tau_3^* \\ \tau_4^* \\ \tau_5^* \end{bmatrix} = \begin{bmatrix} \tau_1 \\ \tau_2 - \tau_3 \\ \tau_3 - \tau_4 \\ \tau_4 - \tau_5 \\ \tau_5 \end{bmatrix} \qquad (42)$$

The inertias of the chain-wheel sets can be treated the same way as the belts and pulleys of the first example. With known motions and inertial properties of the coupling links, we can solve the dynamic equilibrium of the links in the two parallelograms shown in Fig. 5 (with links not marked with × treated as massless). This gives us the additional torques $\Delta\tau_1^*$, $\Delta\tau_2^*$ and $\Delta\tau_3^*$ needed for balancing the inertial forces and moments of the coupling links.

5 Conclusion

The conventional methods for computing the joint torques, Jacobian matrix, and compliance matrix are not directly applicable to manipulators with coupled joint motions. This study provides a systematic approach which utilizes the mapping matrix to relate the joint torques, joint speeds, Jacobian matrix, and compliance matrix in one set of generalized coordinates (i.e., the relative joint displacements) to those in another set of generalized coordinates (i.e., the actuator displacements), so that the results obtained with the conventional methods can be easily transformed to the actual ones for coupled manipulators. The method of constructing the mapping matrix presented is derived from the Newton-Euler formulation of manipulator dynamics and it is easy to use. By relating the various parameters using the mapping matrix, the dynamic equations of motion derived for serial manipulators can also be used for coupled manipulators.

6 References

1 Leu, M. C., Dukovski, V., and Wang, K. K., 1987, "Effect of Mechanical Compliance on Deflection of Robot Manipulator," *Annals of the CIRP*, Vol. 36, No. 1, pp. 305–309.

2 Sweet, L. M., and Good, M. C., 1985, "Redefinition of the Robot Control Problem: Effects of Plant Dynamics, Drive System Constraints, and User Requirements," *IEEE Conference on Decision and Control*, Las Vegas.

3 Asada, H., and Slotine, J.-J. E., 1986, *Robot Analysis and Control*, Chapter 4, John Wiley and Sons, New York.

4 Paul, R. P., 1981, *Robot Manipulator: Mathematics, Programming and Control*, MIT Press, Cambridge, MA.

5 Craig, J. J., 1986, *Introduction to Robotics: Mechanics & Control*, Reading, MA.

6 Fu, K. S., Gonzalez, R. C., and Lee, C. S. G., 1987, *Robotics: Control, Sensing, Vision, and Intelligence*, McGraw-Hill, New York.

7 Orin, D. E., and Schrader, W. W., 1984, "Efficient Computation of the Jacobian for Robot Manipulators," *International Journal of Robotics Research*, Vol. 3, No. 4, pp. 66–75.

8 Whitney, D. E., 1972, "The Mathematics of Coordinated Control of Prosthetic Arms and Manipulators," ASME *Journal of Dynamic Systems, Measurements, and Control*, Vol. 122, pp. 303–309.

9 Luh, J. Y. S., and Zheng, Y.-F., 1985, "Computation of Input Generalized Forces for Robots with Closed Kinematic Chain Mechanisms," *IEEE Journal of Robotics and Automation*, Vol. RA-1, No. 2, pp. 95–103.

10 Freudenstein, F., and Yang, A. T., 1972, "Kinematics and Statics of a Coupled Epicyclic Spur-Gear Train," *Journal of Mechanisms and Machine Theory*, Vol. 7, pp. 263–275.

11 Freudenstein, F., Longman, R. W., and Chen, C.-K., 1984, "Kinematic Analysis of Robotic Bevel-Gear Trains," ASME JOURNAL OF MECHANISMS, TRANSMISSIONS, AND AUTOMATION IN DESIGN, Vol. 106, pp. 371–375.

12 Tsai, L.-W., 1988, "The Kinematics of Spatial Robotic Bevel-Gear Trains," *IEEE Journal of Robotics and Automation*, Vol. 4, No. 2, pp. 150–156.

13 Chang, S.-L., and Tsai, L.-W., 1989, "Synthesis and Analysis of Geared Robotic Mechanisms," *IEEE International Conference on Robotics and Automation*, Scottsdale, AZ, pp. 920–927.

14 Leaver, S. O., and McCarthy, J. M., 1987, "The Design of Three Jointed Two-Degree-of-Freedom Robot Fingers," *ASME Advances in Design Automation*, DE-10, Vol. 2, pp. 127–133.

15 Tsai, L.-W., and Lee, J.-J., 1989, "Kinematic Analysis of Tendon-Driven Robotic Mechanisms Using Graph Theory," ASME JOURNAL OF MECHANISMS, TRANSMISSIONS, AND AUTOMATION IN DESIGN, Vol. 111, pp. 59–65.

16 Morecki, A., Buśko, Z., Gasztold, H., and Jaworek, K., 1980, "Synthesis and Control of the Anthropomorphic Two-Handed Manipulator," *Proceedings of Tenth International Symposium on Industrial Robots*, Milan, Italy.